The RSOS model for a slit with different walls

2003 J. Phys. A: Math. Gen. 36 4551

(http://iopscience.iop.org/0305-4470/36/16/306)

INSTITUTE OF PHYSICS PUBLISHING JOURNAL OF PHYSICS A: MATHEMATICAL AND GENERAL
J. Phys. A: Math. Gen. **36** (2003) 4551–4559 PII: S0305-4470(03)58984-3

The RSOS model for a slit with different walls

B Różycki and M Napiórkowski

Instytut Fizyki Teoretycznej, Uniwersytet Warszawski, Hoża 69, 00 681 Warszawa, Poland

Received 30 January 2003, in final form 5 March 2003
Published 8 April 2003
Online at stacks.iop.org/JPhysA/36/4551

Abstract
An interface fluctuating between two different, parallel, and competing walls separated by distance L is analysed within the framework of the one-dimensional restricted solid-on-solid model. For finite L-values the analytic expressions representing scaling behaviour of the free-energy density and the parallel correlation length are derived and discussed. For infinite wall separation the interface can be located either at finite or at infinite distance from a selected wall. We find that both first- and second-order transitions between these two configurations are possible.

PACS numbers: 68.08.Bc, 68.18.Jk

1. Introduction

The second-order wetting transition taking place in a semi-infinite system bounded by a planar substrate is related to non-analytic behaviour of the surface free-energy density [1–3]. Upon varying the state of the system along the bulk α–β coexistence line, the thickness of the β-like layer entering between the substrate and the phase α becomes macroscopically large at the transition; the α–β interface depins continuously from the substrate.

If the system is made finite along the direction perpendicular to the substrate by adding a second wall, parallel to the first one, and placed at a distance L from it (the slit geometry) then the properties of the system become modified with respect to the semi-infinite case [4–6]. In particular, the surface free-energy density is analytic and additionally depends on the distance L. The walls bounding the system can by chosen in such a way that the lower one preferentially adsorbs phase β and the upper one adsorbs phase α (see figure 1). Such systems were studied intensively [7] using mean-field theory [8, 9], computer simulations [10, 11] and exactly solvable models [12]. In particular, the finite-size scaling functions for the surface free-energy density and for the longitudinal correlation length were found using the one-dimensional solid-on-solid (SOS) model [12] in the case when the interactions of the interface with each wall were identical.

The main purpose of this paper is to analyse the case when the interaction of the interface with each wall is different. We want to see to what extent the difference in wall properties influences—qualitatively and quantitatively—the behaviour of the system.

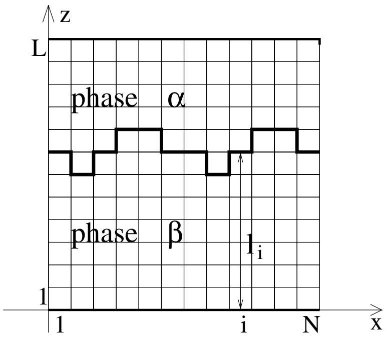

Figure 1. The one-dimensional RSOS model. The position of the α–β interface above the ith site is denoted by l_i. The walls are placed at $z = 0$ and $z = L$.

For this purpose we analyse the one-dimensional SOS model [12–19], see figure 1, in which the position of the interface separating the phases α and β is the only relevant degree of freedom. It is specified by the set of discrete variables l_n, where $n = 1, 2, \ldots, N$ measures the discrete distance along the one-dimensional walls located at $z = 0$ and $z = L$. Each of the N variables l_n can take $L + 1$ values: $l_n \in \{0, \ldots, L\}$. The interaction of the interface with the walls is described by the contact potential

$$\Phi(\{l_i\}_{i=1,\ldots,N}) = \sum_{n=1}^{N} V(l_n) = \sum_{n=1}^{N} \left[-W_1\delta_{l_n,0} - W_2\delta_{l_n,L}\right] \tag{1}$$

which is parametrized by the interaction energies $W_1 > 0$ and $W_2 > 0$ at the lower and upper walls, respectively. The Hamiltonian of the SOS model

$$H(\{l_i\}) = \sum_{n=1}^{N} [J\,|l_n - l_{n+1}| + V(l_n)] \tag{2}$$

contains—in addition to the potential energy—the term describing the energetic cost due to corrugation of the interface; $J > 0$ is a coupling parameter corresponding to the surface tension. We impose the periodic boundary conditions along the walls, i.e., $l_{N+1} = l_1$. Additionally, we assume that the interfacial positions at the neighbouring sites differ at most by one, i.e., $|l_{k+1} - l_k| \in \{0, 1\}$. This assumption means that the interface does not fluctuate too violently and it corresponds to the condition $|\nabla\ell|^2 \ll 1$ often imposed on continuum models. In this way one arrives at the so-called restricted solid-on-solid model (RSOS) [15] which is the object of our analysis.

We recall that the RSOS model of a semi-infinite system bounded by a single wall at $z = 0$ and described by the Hamiltonian

$$H_{\infty/2}(\{l_i\}) = \sum_{n=1}^{N} \left[J\,|l_n - l_{n+1}| - W\delta_{l_n,0}\right] \tag{3}$$

exhibits the second-order wetting transition [15, 19]. It takes place at the wetting temperature T_W given implicitly by the equation [14, 15]

$$w_0 = \frac{1 + 2j_0}{1 + j_0} \tag{4}$$

where $w_0 = \exp(W/k_BT_W)$ and $j_0 = \exp(-J/k_BT_W)$. The average position of the interface $\langle l_k\rangle$ diverges at the wetting temperature as $\langle l_k\rangle \sim |T - T_W|^{-1}$ ($\beta_S = 1$), the free-energy density is non-analytic, i.e., its second derivative with respect to temperature is discontinuous ($\alpha_S = 0$), and the height–height correlation length $\xi_\parallel$ diverges as $\xi_\parallel \sim |T - T_W|^{-2}$ ($\nu_\parallel = 2$). The above results represent the correct low-temperature limit of the two-dimensional Ising model properties [16, 17].

In the model of a slit considered in this paper there are two characteristic temperatures T_{W1} and T_{W2}. Each of them corresponds to critical wetting taking place in an appropriate semi-infinite system bounded by a single wall.

2. The transfer matrix method

A very convenient way of analysing the RSOS model is provided by the transfer-matrix method [14]. In the present case the transfer matrix £ has dimension $L + 1$ and its elements take the form

$$\langle m|£|n\rangle = \exp\left[-\frac{1}{k_B T}\left(J\,|m-n| + \frac{1}{2}V(m) + \frac{1}{2}V(n)\right)\right]. \tag{5}$$

The transfer matrix is symmetric $£ = £^T$ and there exists an orthonormal basis $\{|\Psi_i\rangle\}_{i=0,\dots,L}$ consisting of its eigenvectors. The real eigenvalues λ_i are numbered in such a way that $\lambda_0 \geqslant \lambda_1 \geqslant \cdots \geqslant \lambda_L$. For periodic boundary condition the partition function $Z(T, N)$ can be evaluated in the standard way

$$Z(T,N) = \sum_{\{l_i\}} \mathrm{e}^{-\frac{H(\{l_i\})}{k_B T}} = \sum_{\{l_i\}} \prod_{n=1}^{N} \langle l_n|£|l_{n+1}\rangle = \sum_{l_1=0}^{L} \langle l_1|£^N|l_1\rangle = \sum_{k=0}^{L} (\lambda_k)^N \tag{6}$$

and leads in the thermodynamic limit $N \to \infty$ to the free energy per site f

$$f \equiv -k_B T \lim_{N\to\infty}\left[\frac{1}{N}\log Z(T,N)\right] = -k_B T \log\lambda_0 \tag{7}$$

together with the parallel correlation length $\xi_\parallel$

$$\xi_\parallel = \left[\log\left(\frac{\lambda_0}{\lambda_1}\right)\right]^{-1} \tag{8}$$

and the mean location of the interface

$$\langle l_k\rangle \equiv \lim_{N\to\infty} \frac{1}{Z(T,N)} \sum_{\{l_i\}} l_k\, \mathrm{e}^{-\frac{H(\{l_i\})}{k_B T}} = \sum_{l_k=0}^{L} l_k |\Psi_0(l_k)|^2 \tag{9}$$

where $\Psi_0(l)$ is the lth component of the eigenvector corresponding to the largest eigenvalue λ_0. The mean position of the interface $\langle l\rangle \equiv \langle l_k\rangle$ does not depend on the site number k. It follows from equation (9) that the function $P(l) = |\Psi_0(l)|^2$ represents the probability of finding the interface at distance l from the lower wall. We analyse its properties in the next chapter.

3. The solution of the RSOS model and the scaling functions

The RSOS model constraint $|l_{k+1} - l_k| \in \{0, 1\}$ and the form of the contact potential $\Phi(\{l_k\})$, see equation (1), lead to the following expressions for the transfer matrix elements

$$\langle m|£|n\rangle = \begin{cases} j^{|m-n|} w_1^{\frac{1}{2}\delta_{m,0}+\frac{1}{2}\delta_{n,0}} w_2^{\frac{1}{2}\delta_{m,L}+\frac{1}{2}\delta_{n,L}} & \text{for} \quad |m-n| \in \{0,1\} \\ 0 & \text{otherwise} \end{cases} \tag{10}$$

where $w_1 = \mathrm{e}^{W_1/k_B T}$, $w_2 = \mathrm{e}^{W_2/k_B T}$ and $j = \mathrm{e}^{-J/k_B T}$. The solutions of the eigenvalue equation $£|\Psi_k\rangle = \lambda_k|\Psi_k\rangle$ can be found along the lines described in [12, 15]. Both the

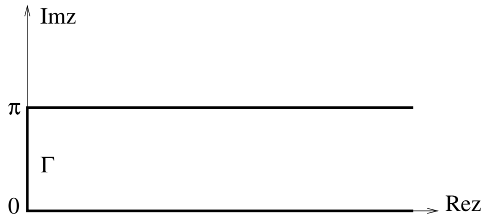

Figure 2. The contour Γ on which the values of parameters z_k are located.

eigenvalues λ_k and the eigenvectors $\Psi_k(l)$ are obtained as functions parametrized by $(L+1)$ auxiliary variables z_k which are roots of the equation $\det[\mathbb{A}(z)] = 0$, where $\mathbb{A}$ is a 2×2 matrix

$$\mathbb{A} = \begin{bmatrix} w_1(1+j\,\mathrm{e}^{-z}) - (1+2j\cosh z) & w_1(1+j\,\mathrm{e}^{z}) - (1+2j\cosh z) \\ (w_2(1+j\,\mathrm{e}^{z}) - (1+2j\cosh z))\,\mathrm{e}^{-zL} & (w_2(1+j\,\mathrm{e}^{-z}) - (1+2j\cosh z))\,\mathrm{e}^{zL} \end{bmatrix}. \tag{11}$$

The transfer matrix eigenvalues λ_k are given by the equation

$$\lambda_k = 1 + 2j\cosh z_k \tag{12}$$

and the eigenvector $\Psi_0(l)$ takes the form

$$\Psi_0(l) = c(l)\left[a_0\,\mathrm{e}^{-z_0 l} + b_0\,\mathrm{e}^{z_0 l}\right] \tag{13}$$

where

$$c(l) = \begin{cases} w_1^{-1/2} & \text{for} \quad l = 0 \\ 1 & \text{for} \quad l = 1,\ldots,L-1\,. \\ w_2^{-1/2} & \text{for} \quad l = L \end{cases}$$

The parameters a_0 and b_0 in equation (13) are determined by the equation $\mathbb{A}(z_0)[a_0, b_0]^T = [0, 0]^T$ and the normalization condition $\sum_{l=0}^{L}|\Psi_0(l)|^2 = 1$. Equation (12) implies that $z_k \in \Gamma$, where the contour Γ is shown in figure 2. It follows from the condition $z_k \in \Gamma$ that

- for real $z_k \in [0, \infty[$ the eigenvalues $\lambda_k \geqslant 1 + 2j$,
- for imaginary $z_k = \mathrm{i}|z_k|$, where $|z_k| \in\,]0, \pi[$, the eigenvalues $\lambda_k \in\,]1-2j, 1+2j[$,
- for complex $z_k = \mathrm{i}\pi + r_k$, where $r_k \in [0, +\infty[$, the eigenvalues $\lambda_k \leqslant 1 - 2j$.

The probability distribution $P(l) = |\Psi_0(l)|^2$ takes—provided $a_0 \neq 0$ and $b_0 \neq 0$, see equation (13)—the following form

$$P(l) = 4c(l)^2|a_0 b_0|\cosh^2(z_0(l - \bar{l})) \tag{14}$$

where

$$\bar{l} = \frac{1}{2z_0}\log\frac{a_0}{b_0}. \tag{15}$$

The parameters a_0 and b_0 depend on the distance L between the walls and on parameter z_0. The probability distribution $P(l)$ is either a concave or a convex function. This property depends on the value of parameter z_0 and changes at $z_0 = 0$, i.e., for $z_0 \to 0$ along the real axes the distribution $P(l)$ is convex while for $z_0 \to 0$ along the imaginary axes it is concave. Thus the condition $z_0 = 0$ determines a characteristic temperature $T^\star$ at which the probability distribution $P(l)$ turns from being convex to concave. In the case of equal wall interaction energies $W_1 = W_2 \equiv W$—which was analysed by Privman and Švrakić [12]—the temperature $T^\star$ is equal to the wetting temperature T_W given by equation (4). In order to analyse the properties of the system in the vicinity of $T^\star$ with the help of the analytical methods we assume that the wetting temperatures of the walls are close to each other, i.e., $|T_{W1} - T_{W2}|/T_{W1} \ll 1$. Expanding the lhs of equation $\det[\mathbb{A}(z)] = 0$ (which determines the set of variables z_k) in small parameters $\tau_1 = (T - T_{W1})/T_{W1}$, $\tau_2 = (T - T_{W2})/T_{W2}$ and $z \to 0$, one obtains

$$z^2 + \mu_1\mu_2 = (\mu_1 + \mu_2)z \coth(Lz) \tag{16}$$

where the parameters μ_1 and μ_2 are defined as

$$\mu_k = \frac{w_k(1 + j) - (1 + 2j)}{j w_k} \approx -a_k\tau_k \tag{17}$$

$k \in \{1, 2\}$. The constant parameters $a_k > 0$ do not depend on the temperature. A straightforward analysis of equation (16) shows that it has at most two roots which may be real and positive; they are denoted as z_0 and z_1. The remaining roots $z_2, \ldots, z_L$ are always imaginary. Whether the first two roots are real or imaginary depends on the values of μ_1, μ_2 and L. This implies, see equation (12), that there are only two eigenvalues which can be larger than $1 + 2j$

$$\lambda_i = 1 + 2j + jz_i^2 \qquad \text{for} \quad z_i \to 0 \tag{18}$$

$i \in \{0, 1\}$, while the remaining ones are always smaller than $1 + 2j$.

In order to extract the scaling behaviour of the free-energy density and the parallel correlation length it is convenient to introduce the scaling parameters $x_k \equiv -L\mu_k = a_k\tau_k L$, $y \equiv L^2z^2$, and to rewrite equation (16) in the following way:

$$y + x_1x_2 + (x_1 + x_2)\sqrt{y}\coth(\sqrt{y}) = 0. \tag{19}$$

There are two solutions of the above equation which can be either positive or negative depending on the values of the parameters x_1, x_2; they are denoted as $y_0(x_1, x_2) = L^2z_0^2$ and $y_1(x_1, x_2) = L^2z_1^2$. It follows from equation (18) that in the limit $z_0 \to 0$ the free-energy density, equation (7), can be written as the sum of two terms $f = f_0 + \delta f$, where the L-independent term $f_0 = -k_BT\log(1 + 2j)$ represents the free-energy density of the free interface, and the second term incorporates the interaction of the interface with the walls

$$\delta f = -\frac{k_BTj}{1 + 2j}\frac{y_0(a_1\tau_1L, a_2\tau_2L)}{L^2}. \tag{20}$$

Similarly, using equations (8) and (18) one can find the parallel correlation length in the limit $z_0 \to 0$ and $z_1 \to 0$

$$\xi_\parallel = \frac{1 + 2j}{j}\frac{L^2}{y_0(a_1\tau_1L, a_2\tau_2L) - y_1(a_1\tau_1L, a_2\tau_2L)}. \tag{21}$$

The two largest solutions of equation (19), i.e., $y = y_0(x_1, x_2)$ and $y = y_1(x_1, x_2)$, represent the finite-size scaling functions. They are both analytic at the origin and after expanding in powers of x_1 and x_2 one obtains

$$y_0(x_1, x_2) = -(x_1 + x_2) + \tfrac{1}{3}\left(x_1^2 + x_2^2 - x_1x_2\right) + \cdots \tag{22}$$

and

$$y_1(x_1, x_2) = -\pi^2 - 2(x_1 + x_2) + \frac{1}{\pi^2}(x_1 + x_2)^2 + \cdots. \tag{23}$$

In the range of model parameters where equations (22) and (23) are valid, i.e., for $|\tau_1|L \ll 1$ and $|\tau_2|L \ll 1$, the finite-size contribution to the free-energy density (20) becomes proportional to $\delta f \sim \frac{\mu_1+\mu_2}{L}$. The parallel correlation length (21) is finite and scales with the distance L as $\xi_\parallel \sim L^2$. On the other hand, solving equation (19) for $x_1, x_2 \to -\infty$ one finds

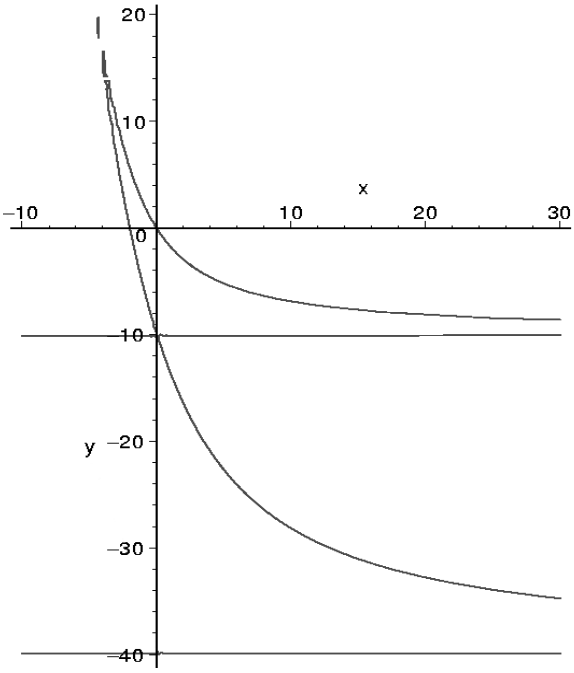

Figure 3. The scaling functions $y_0(x)$ and $y_1(x)$ for the case $W_1 = W_2$. The horizontal lines correspond to the asymptotes $y = -\pi^2$ and $y = -4\pi^2$.

$y_0 = \max\left(x_1^2, x_2^2\right)$ and $y_1 = \min\left(x_1^2, x_2^2\right)$. This regime corresponds to the limit $L \to \infty$ which will be discussed in the next section.

In the case of identical wall parameters $W_1 = W_2$ one has $T_{W1} = T_{W2}, x_1 = x_2$, and equation (19) reduces to the following form:

$$\left(x_1 + \sqrt{y}\tanh\left(\tfrac{1}{2}\sqrt{y}\right)\right)\left(x_1 + \sqrt{y}\coth\left(\tfrac{1}{2}\sqrt{y}\right)\right) = 0. \tag{24}$$

The two largest solutions of the above equation, $y_0(x_1)$ and $y_1(x_1)$, are implicitly given by the following relations:

$$x_1 = -\sqrt{y_0}\tanh\left(\tfrac{1}{2}\sqrt{y_0}\right) \qquad \text{for} \quad y_0 > -\pi^2 \tag{25}$$

and

$$x_1 = -\sqrt{y_1}\coth\left(\tfrac{1}{2}\sqrt{y_1}\right) \qquad \text{for} \quad y_1 > -4\pi^2. \tag{26}$$

The plots of the above scaling functions are shown in figure 3 and reproduce the results already derived by Privman and Švrakić [12].

In the case $W_1 \neq W_2$, for fixed values of the wetting temperatures T_{W1}, T_{W2}, and the distance L the reduced variables x_k are parametrized by the temperature T only and are related by the linear equation $x_2 = px_1 + q$, where $p = \frac{a_2 T_{W1}}{a_1 T_{W2}}$ and $q = \frac{T_{W1} - T_{W2}}{T_{W2}} a_2 L$. The plots of the scaling functions $y_0(x_1, px_1 + q)$ and $y_1(x_1, px_1 + q)$ are shown in figure 4. From comparing figures 4 and 3 one notes that the scaling functions y_0 and y_1 differ qualitatively in both cases. If $W_1 = W_2$ then the difference $(y_0 - y_1) \to 0$ for $x_1 \to -\infty$ and—as was proved in [12]—the correlation length (21) diverges exponentially with the distance L in this limit, i.e., $\xi_\parallel \sim \mu_1^{-2}\exp(|\mu_1|L)$ for $\mu_1 L \gg 1$. For the $W_1 \neq W_2$ case the difference $y_0 - y_1$ behaves differently and one has $\lim_{x_1 \to -\infty}(y_0 - y_1) \neq 0$. One also notes that $y_0(x_1 = 0) = 0$ for $W_1 = W_2$ while for the other case $y_0(x_1, px_1 + q) = 0$ for $x_1 \neq 0$. The condition $y_0 = 0$

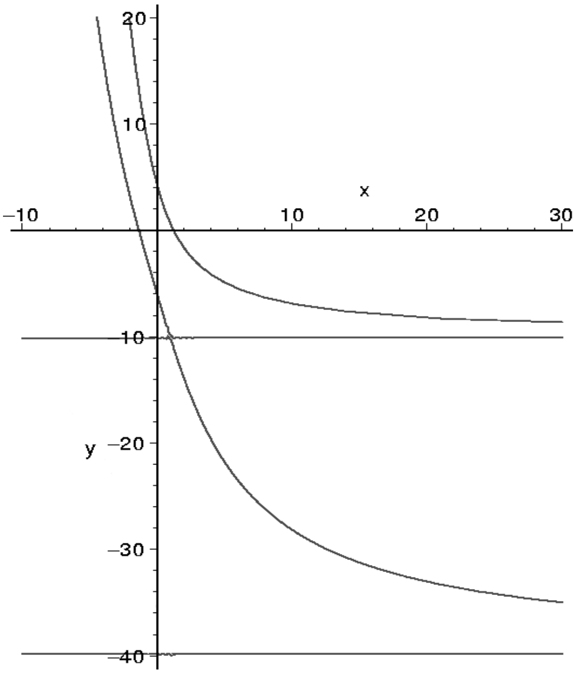

Figure 4. The scaling functions $y_0(x, px + q)$ and $y_1(x, px + q)$ for the case $W_1 \neq W_2$; $p = 1.2$ and $q = -2$. The horizontal lines correspond to the asymptotes $y = -\pi^2$ and $y = -4\pi^2$.

implies $z_0 = 0$ and determines the temperature $T^\star$ at which the probability distribution $P(l)$ changes its convexity. Thus for $W_1 = W_2$ the temperature $T^\star = T_{W1} = T_{W2}$ while for $W_1 \neq W_2$ one has $T^\star \neq T_{W1}$ and $T^\star \neq T_{W2}$. It follows from equation (19) that $T = T^\star$ corresponds to $x_1 + x_2 + x_1 x_2 = 0$. From this equation the expression for $T^\star$ is obtained which for $1/L \ll 1$ takes the form

$$T^\star = \max\left[T_{W1}\left(1 - \frac{1}{a_1 L}\right), T_{W2}\left(1 - \frac{1}{a_2 L}\right)\right] + O\left(\frac{1}{L^2}\right). \tag{27}$$

It follows from equation (20) that for $T = T^\star$ the finite-size contribution to the free-energy density δf vanishes. Simultaneously the effective interaction between the walls mediated by the fluctuations vanishes. The characteristic temperature $T^\star$ is shifted with respect to the larger of the wetting temperatures $T_W^+ = \max(T_{W1}, T_{W2})$. This shift—for $1/L \ll 1$—scales with the distance L according to the following relation: $(T_W^+ - T^\star)/T_W^+ \sim L^{-1}$. Because for the present model the critical exponent $\beta_S = 1$ this result is in accordance with the general prediction for a slit with competing walls [9].

4. The phase diagram for the case $L = \infty$

In the limiting case $L = \infty$ there exists an infinite number of imaginary solutions to equation (16) which are contained in the segment $[0, i\pi] \subset \Gamma$. However, we are interested in real and positive values of $z \in \mathbb{R}^+$. In this case equation (16) simplifies to the following form:

$$(z - \mu_1)(z - \mu_2) = 0. \tag{28}$$

The above equation (28) has no solution if $\max(\mu_1, \mu_2) < 0$. If $\mu_1 \geqslant \mu_2$ and $\mu_1 > 0$ then $z_0 = \mu_1$. For $z_0 = \mu_1$ the parameter b_0 vanishes and the probability distribution $P(l)$ decays

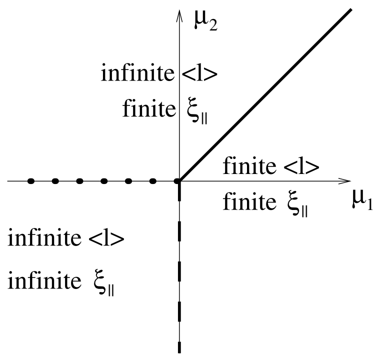

Figure 5. The phase diagram in the $L = \infty$ case. The solid line indicates the first-order transition points. The vertical dashed line is the second-order transition line. Upon crossing the horizontal dotted line towards negative values of μ_2 the correlation length $\xi_\parallel$ becomes infinite while the average distance of the interface from the lower wall remains infinite.

exponentially: $P(l) = c^2(l)|a_0|^2\,\mathrm{e}^{-2l\mu_1}$. In this case the average distance of the interface from the lower wall is finite. If $\mu_2 > \mu_1$ and $\mu_2 > 0$ then $z_0 = \mu_2$. In this case the distribution $P(l)$ is given by equation (14), i.e., $P(l) = 4c^2(l)|a_0 b_0|\cosh^2(\mu_2(l - \bar{l}))$ for a finite value of $\bar{l}$, see equation (15), and the mean distance $\langle l \rangle$ is infinite. Thus the line $\mu_1 = \mu_2$ (the solid line in figure 5) corresponds to the first-order transitions at which the interface unbinds from the lower wall and becomes pinned to the upper one. On the other hand, upon crossing the line $\mu_1 = 0$, $\mu_2 < 0$ (the dashed line in figure 5) from $\mu_1 \to 0^+$, where the probability distribution is equal to $P(l) = c^2(l)|a_0|^2\,\mathrm{e}^{-2l\mu_1}$, the mean value $\langle l \rangle$ diverges continuously; it corresponds to the second-order interface unbinding transition taking place at the wetting temperature of the lower wall T_{W1}. Thus upon changing the model parameters μ_1 and μ_2 both first- and second-order transitions are possible. Our conclusion about the existence of the first-order transitions in the limiting case $L = \infty$ recalls the prediction of Forgacs *et al* [13] where the first-order interface unbinding transition in a semi-infinite geometry bounded by a single substrate and containing the line of defects at the distance L from it was found in the limit $L \to \infty$. However, it should be noted that upon varying only the temperature T in the regime $T \to T_{W1}$ and $T \to T_{W2}$ at fixed values of the wetting temperatures T_{W1} and T_{W2} (or, equivalently, at fixed values of the Hamiltonian parameters W_1, W_2 and J) only the second-order unbinding transition is possible and it takes place at $T = T_{W1}$. It corresponds to the wetting transition in the single-wall case.

Using equations (8) and (16) one can also find the parallel correlation length which takes the form

$$\xi_\parallel = \frac{1+2j}{j}\left|\mu_1^2\Theta(\mu_1) - \mu_2^2\Theta(\mu_2)\right|^{-1} \tag{29}$$

where Θ is the Heaviside function. The parallel correlation length $\xi_\parallel$ diverges both at the first-order transition line $\mu_1 = \mu_2$, where $\xi_\parallel \sim |\mu_1 - \mu_2|^{-1}$, and at the second-order transition line, where $\xi_\parallel \sim \mu_1^{-2}$. It is infinitely large for $\mu_1 \leqslant 0$ and $\mu_2 \leqslant 0$ (see figure 5).

5. Summary

We have presented the analytic solution of the one-dimensional RSOS model of an interface fluctuating between two different, flat, parallel and competing walls separated by distance L. Each of the walls corresponds in the semi-infinite case to the second-order wetting transition characterized by the appropriate wetting temperature, i.e. T_{W1} and T_{W2}. We have investigated the influence of the finite size of the system on the free-energy density and on the height–height correlation length for the case when the two wetting temperatures are close to each other. We found the scaling behaviour of these quantities and the corresponding scaling functions which depend on temperature via the scaling variables $(T - T_{W1})L$, $(T - T_{W2})L$. In the limiting case $L = \infty$ we have constructed the phase diagram in which regions corresponding to finite and infinite values of the mean distance of the interface from the lower wall are indicated. They are separated by transition lines which can be either first- or second-order depending on the choice of system parameters.

Acknowledgment

This work is supported by the Committee for Scientific Research via grant 2PO3B 008 23.

References

[1] de Gennes P G 1985 *Rev. Mod. Phys.* **57** 827
[2] Dietrich S 1988 *Phase Transitions and Critical Phenomena* vol 12 ed C Domb and J L Lebowitz (London: Academic) p 1
[3] Forgacs G, Lipowsky R and Nieuwenhuizen Th M 1991 *Phase Transitions and Critical Phenomena* vol 14 ed C Domb and J L Lebowitz (London: Academic) p 135
[4] Barber M 1983 *Phase Transitions and Critical Phenomena* vol 8 ed C Domb and J L Lebowitz (London: Academic) p 145
[5] Privman V 1990 *Finite-Size Scaling and Numerical Simulation of Statistical System* ed V Privman (Singapore: World Scientific) p 1
[6] Krech M 1994 *The Casimir Effect in Critical Systems* (Singapore: World Scientific)
[7] Binder K and Luijten E 2001 *Phys. Rep.* **344** 179
[8] Lipowsky R and Gompper G 1984 *Phys. Rev.* B **29** 5213
[9] Parry O A and Evans R 1990 *Phys. Rev. Lett.* **64** 439
[10] Binder K, Landau D P and Ferrenberg A M 1995 *Phys. Rev. Lett.* **74** 298
[11] Binder K, Landau D P and Ferrenberg A M 1995 *Phys. Rev.* E **51** 2823
[12] Privman V and Švrakić N M 1988 *Phys. Rev.* B **37** 3713
[13] Forgacs G, Švrakić N M and Privman V 1988 *Phys. Rev.* B **37** 3818
Forgacs G, Švrakić N M and Privman V 1988 *Phys. Rev.* B **38** 8996
[14] Chui S T and Weeks J D 1981 *Phys. Rev.* B **23** 2438
[15] Swain P S and Parry A O 1997 *J. Phys. A: Math. Gen.* **30** 4597
[16] Abraham D B 1980 *Phys. Rev. Lett.* **44** 1165
[17] Chalker J T 1981 *J. Phys. A: Math. Gen.* **14** 2431
[18] Burkhardt T W 1981 *J. Phys. A: Math. Gen.* **14** L63
[19] Burkhardt T W 1988 *J. Phys. A: Math. Gen.* **31** L549